Supplement of Atmos. Meas. Tech., 19, 3481–3490, 2026
https://doi.org/10.5194/amt-19-3481-2026-supplement

Atmospheric Measurement Techniques
Open Access
EGU

Supplement of

Characterization of a portable, light-weight, low-power chemical ionization time-of-flight mass spectrometer

Austin D. Dobrecevich et al.

Correspondence to: Joel A. Thornton (joelt@uw.edu)

Table S1: 13-Component VOC mixture in nitrogen. Concentrations displayed are accurate to 10%.

Standard	**Compound CAS#**	**Concentration (*ppbv*)**
Methanol	67-56-1	1000
Acetonitrile	70-05-8	1000
Acetaldehyde	75-07-0	1000
Acrylonitrile	107-13-1	1000
Acetone	67-64-1	1000
Isoprene	78-79-5	1000
Methyl Ethyl Ketone	78-93-3	1000
Benzene	71-43-2	1000
Toluene	108-88-3	1000
m-Xylene	108-38-3	1000
1,2,4-Trimethylbenzene	95-63-6	1000
α-Pinene	80-56-8	1000
β-Caryophyllene	87-44-5	100

Table S2: Measured and Calculated Analyte Sensitivities of the AIM reactor in $[I]^-$ mode. These sensitivities were reported in the literature for the AIM IMR operated at 50 mbar (Aggarwal et al., 2025; Riva et al., 2024; Wang et al., 2026). The AIM inlet in our experiments for the Portable-TOF-CIMS was operated at 100 mbar. A sensitivity in [I]- mode was experimentally determined for formic acid (CHOOH) and is shown in the table below as 8.4 ncps/pptv and is bolded. Using the ratio of this as the lower bound and the collision limited sensitivity as the upper bound we calculated the sensitivities of the AIM operated at 100 mbar for the other species we detected in these experiments.

Analyte	Reported Sensitivity @50 mbar (ncps/pptv)	Calculated Sensitivity @100 mbar (ncps/pptv)
HONO	6.5	22.0
HNO3	15.0	30.0
C2H4O2	1.0	3.4
HCOOH	**2.5**	**8.4**
C6H10O5	15.0	30.0
C5H10O3	15.0	30.0

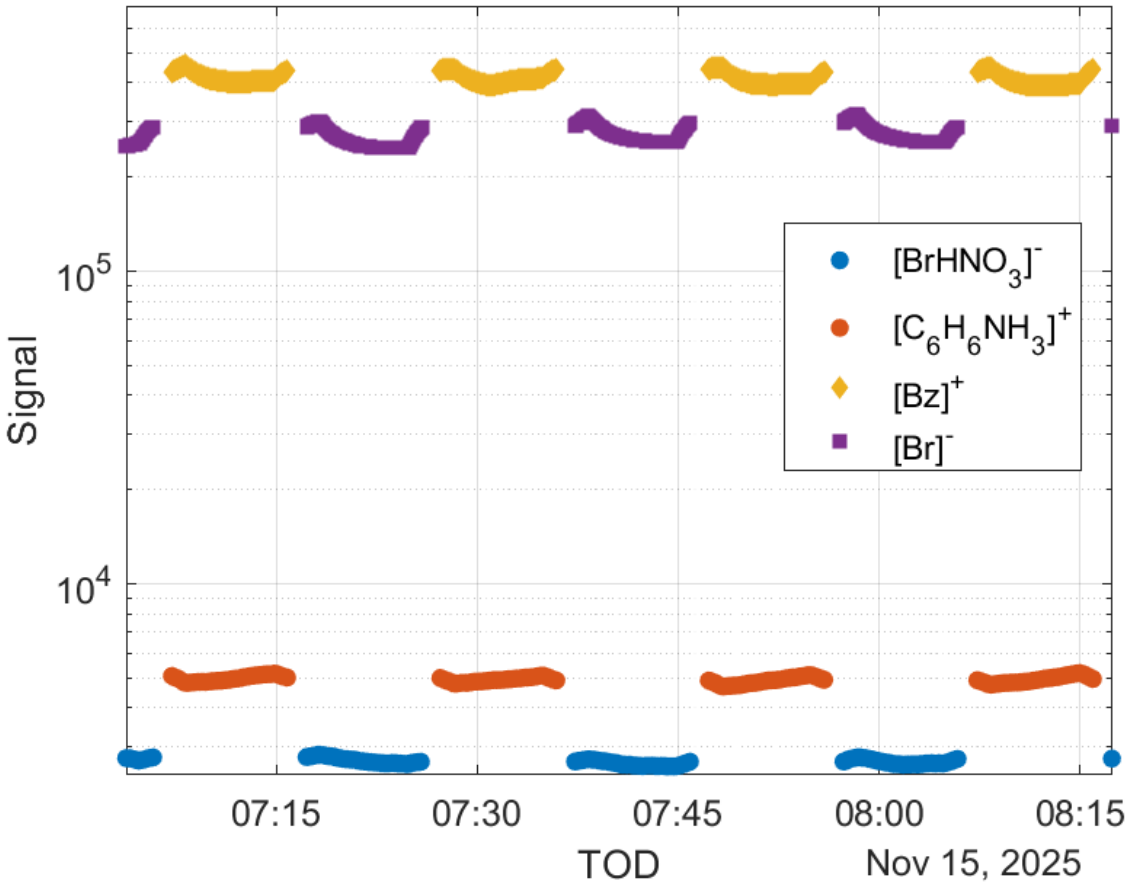

Figure S1: Time-series showing reagent ion switching every 15 minutes from $[Br]^-$ to $[Bz]^+$ and the normalized analyte signals resulting from the different ionization strategies. The reagent ion signals [Bz]+ and [Br]- are plotted in ion counts per second, and the nitric acid and ammonia is plotted in ncps.

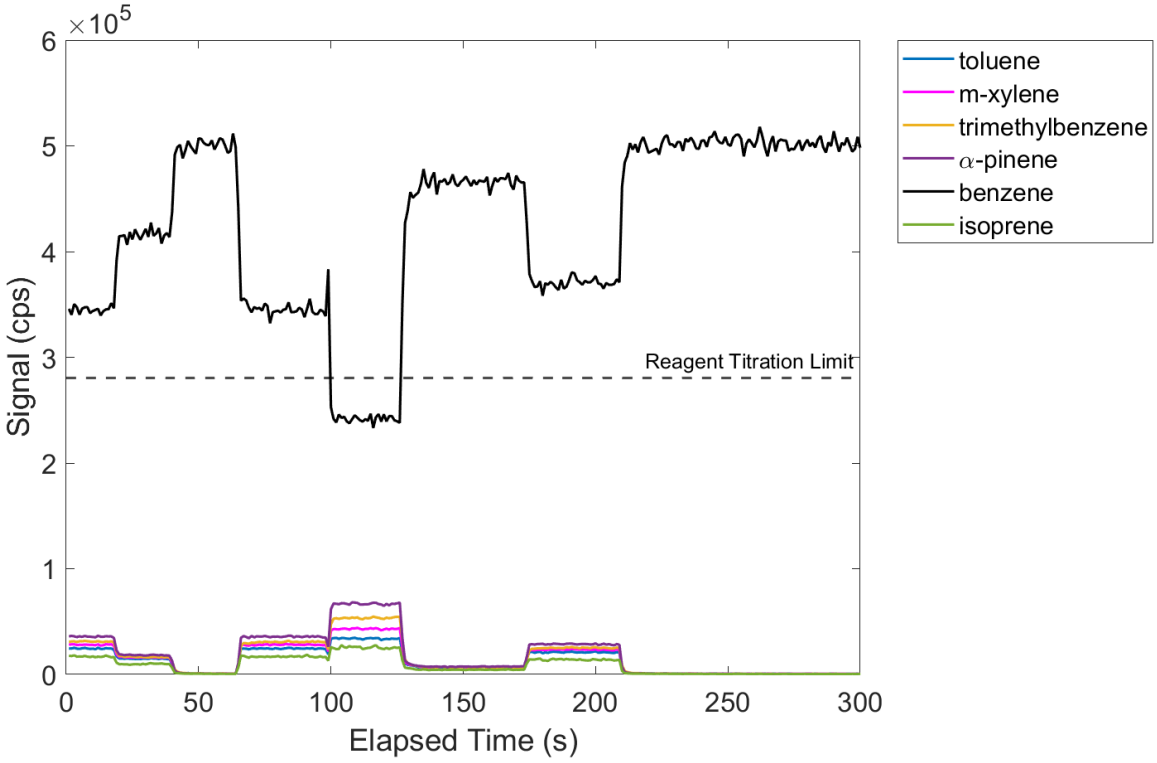

Figure S2: (a) Raw signals recorded during the calibration for the instrument, tracing the $[Bz]^+$ reagent ion signal pre-normalization. (b) Annotated signals to track the abundance of the reagent ion signal while different concentrations of analytes were introduced into the inlet of the AIM reactor.

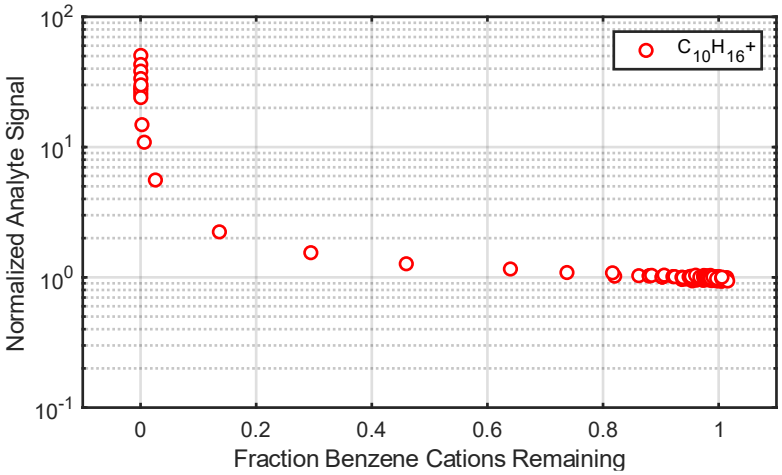

Figure S3: Relationship between resulting analyte signal and fraction of reagent ion remaining for the detection of α-pinene using a [Bz]+ ionization strategy following the introduction of a high concentration of solvent to the inlet to force reagent ion depletion. The resulting normalized analyte signal remains roughly constant until a remaining fraction of 0.5-0.6 remaining after which normalization errors rapidly increase.

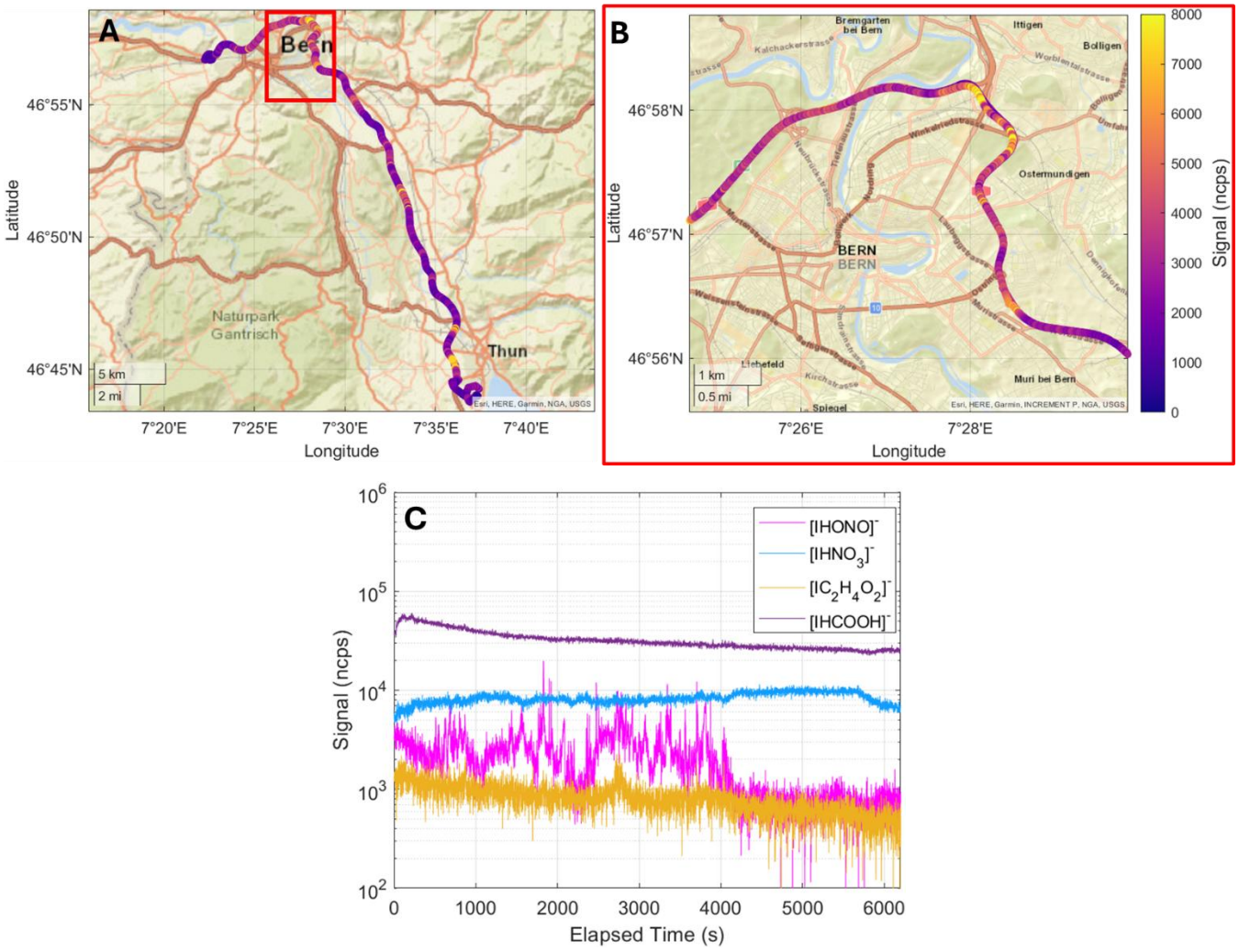

Figure S4: (a) Mobile driving measurements of HONO using iodide chemical ionization detection. (b) Zoom in on area of higher anthropogenic activity tracing HONO. (c) Representative timeseries of different analyte traces during the driving measurements, sensitivities are: 22 ncps/pptv, 30 ncps/pptv, 3.4 ncps/pptv, and 8.4 ncps/pptv for $[IHONO]^-$, $[IHNO_3]^-$. $[IC_2H_4O_2]^-$, $[IHCOOH]^-$, respectively. Further information on sensitivities are shown in Table S2. Sources: Esri, HERE, Garmin, NGA, USGS | Powered by Esri.

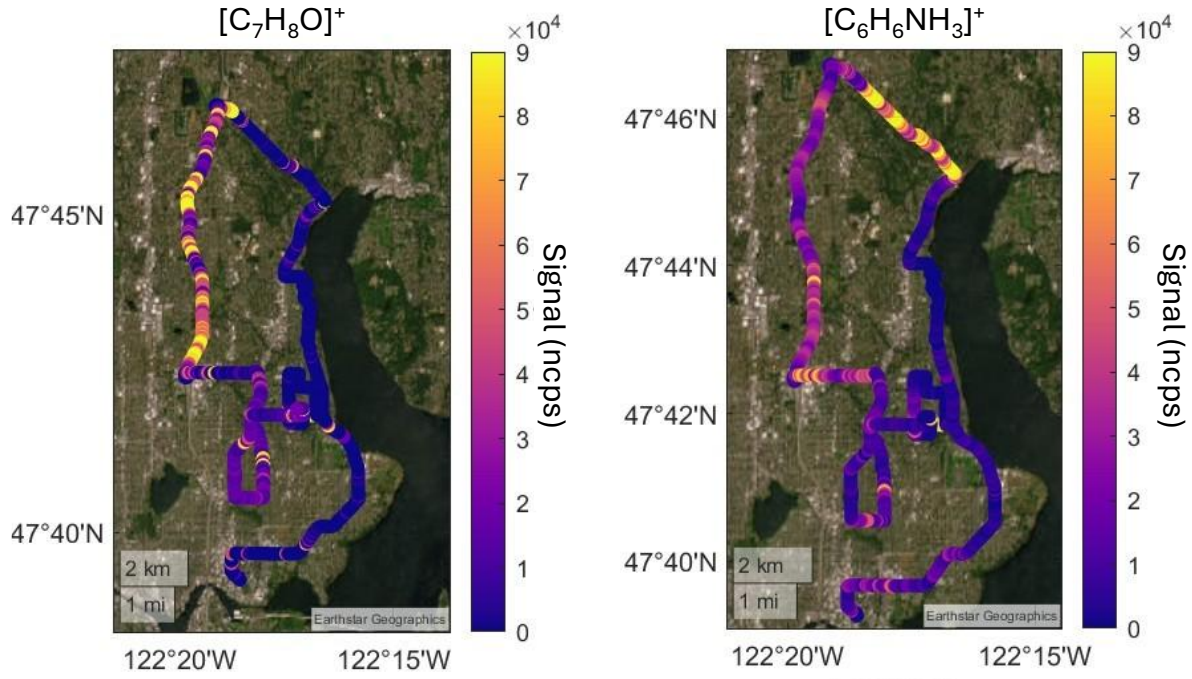

Figure S5: (a) Mobile driving measurements of *m/z* consistent with $C_7H_8O^+$, a suspected woodsmoke tracer using benzene ion chemical ionization detection. (b) Mobile driving measurements of *m/z* consistent with $[NH_3C_6H_6]^+$, the adduct of benzene with ammonia. Both $[C_7H_8O]^+$ and $[C_6H_6NH_3]^+$ are expected to be detected at ~collision limit.

References:

Aggarwal, S., Bansal, P., Wang, Y., Jorga, S., Macgregor, G., Rohner, U., Bannan, T., Salter, M., Zieger, P., Mohr, C., and Lopez-Hilfiker, F.: Identifying key parameters that affect sensitivity of flow tube chemical ionization mass spectrometers, https://doi.org/10.5194/egusphere-2025-696, 6 March 2025.

Riva, M., Pospisilova, V., Frege, C., Perrier, S., Bansal, P., Jorga, S., Sturm, P., Thornton, J. A., Rohner, U., and Lopez-Hilfiker, F.: Evaluation of a reduced-pressure chemical ion reactor utilizing adduct ionization for the detection of gaseous organic and inorganic species, Atmospheric Meas. Tech., 17, 5887–5901, https://doi.org/10.5194/amt-17-5887-2024, 2024.

Wang, Y., Voliotis, A., Matthews, E., Wu, R., Roska, M., Adam, M. G., Dubus, R., Kesper, L., Rohrer, F., Wegener, R., Winter, B., Bates, K. H., He, Q., Hohaus, T., Grasse, A., Tillmann, R., Wahner, A., Wang, H., Wesolek, C., Wedel, S., Wu, Y., Zorn, S. R., Canagaratna, M., Worsnop, D., Lopez-Hilfiker, F., Gkatzelis, G. I., Coe, H., and Bannan, T. J.: Voltage Scanning to Calibrate Multi-Reagent Chemical Ionization Mass Spectrometers (MR-CIMS): From Signal to Sensitivity, https://doi.org/10.5194/egusphere-2025-6102, 19 January 2026.